# Phase Separation Kinetics and Morphology in the Critical to Off-Critical Crossover Region

**Mamoru Okada,*,† Ji Sun,† Jie Tao,† Tsuneo Chiba,‡ and Takuhei Nose†**

*Departments of Polymer Chemistry and of Organic and Polymeric Materials, Tokyo Institute of Technology, Ookayama, Meguro-ku, Tokyo 152, Japan*

*Received May 31, 1995; Revised Manuscript Received July 27, 1995*[⊗]

ABSTRACT: Phase separation kinetics and morphology were studied for polystyrene/poly(2-chlorostyrene) blends containing a small amount of di-*n*-butyl phthalate over a wide composition range by using the time-resolved light scattering technique and electron microscopy. Cocontinuous domains and isolated spherical domains (droplets) were observed to coexist in the critical to off-critical crossover composition region. It was found that the phase-volume fraction was not the only factor determining the crossover compositions. Two maxima corresponding to the scattering from cocontinuous domains and droplets respectively were observed in the scattered light intensity profile. Because of a large difference in the coarsening rate between the two domain structures, only the maximum corresponding to the cocontinuous domains was initially observed. The wavelengths at which the two maxima were located could be expressed by power functions of the phase separation time, and the exponent for each maximum had the same value as in the case where the corresponding domain structure existed separately. This indicated that the coarsening mechanisms of the cocontinuous domains and droplets were scarcely changed by coexistence with the other domain structure.

## Introduction

The kinetics of phase separation of polymer blends has received considerable attention and many theoretical and experimental studies have been made in the past few decades.[1−3] The phase separation process has generally been divided into three stages, namely, the early, the intermediate, and the late stages, and rather different theoretical approaches have been employed to analyze the respective stages.[1−5] The late stage is defined as the stage where microscopic domains (clusters) of coexisting compositions bounded by a sharp interface are formed and phase separation proceeds through coarsening of microdomains with the total volume of each phase being conserved. An important objective of the studies of the phase separation kinetics was controlling the morphological structures of polymer blends through phase separation. Two distinct morphological structures, namely, the cocontinuous domain structure and the isolated spherical domain (droplet) structure, have been known at the late stage of phase separation. The difference in domain structure is reflected in mechanisms of the coarsening of the domain.[6] Especially in fluid mixtures, the presence of continuity among microdomains has an essential importance to the coarsening mechanisms. According to Siggia,[6] when there is a variation in diameter along a tubelike portion of a continuous domain, a gradient of the pressure of the inside fluid is produced along the tube by the interfacial tension and the fluid is driven to flow into a region of larger diameter. This mechanism results in the linear time dependence of the characteristic size of the continuous domain, which makes a marked contrast with the 1/3 power dependence of the characteristic size of droplets that are coarsening by coalescence[7] and the Ostwald ripening mechanisms.[8]

The morphological structure produced by phase separation depends on the location in the phase diagram. At compositions close to the critical point, cocontinuous domains are produced, while at a composition far off the critical point, droplets are produced. Morphological studies of phase-separated domains have been concentrated in these two composition regions (especially in the critical region), and the morphological structure in the intermediate region between the critical and off-critical regions was not well known until we found recently that cocontinuous domains and droplets coexisted in such crossover regions.[9] In that preliminary study, we observed morphological structures at a fixed composition with changing phase separation temperature, and consequently the temperature difference obscured the conclusions drawn for the phase-volume dependence of the morphology. In the present study, we observed the microdomain structures with changing composition at a fixed phase separation temperature to confirm the conclusions in the preliminary report. In addition, we carried out the time-resolved light scattering experiments at the same compositions as the morphology observation was made at in order to elucidate the relation between the morphology and the kinetics in the crossover region.

## Experimental Section

**Materials.** A blend of polystyrene and poly(2-chlorostyrene) containing 10 wt % plasticizer di-*n*-butyl phthalate (DBP) was used as the sample. The present system had a lower critical mixing temperature.[10,11] Polystyrene (PS) was a product of Pressure Chemical Co. with a nominal weight-average molecular weight $M_w = 5.0 \times 10^4$ and polydispersity index $M_w/M_n < 1.06$. Poly(2-chlorostyrene) (P2CS) was obtained by fractionating a product by radical polymerization in toluene with a preparative gel permeation chromatography apparatus. Its molecular weight and polydispersity index were determined by analytic gel permeation chromatography to be $M_w = 9.0 \times 10^4$ and $M_w/M_n = 1.10$.

Thin blend films were prepared by solvent casting from about 3 wt % benzene solution. The films were first dried under atmospheric pressure and then dried under reduced pressure with a gradual increase in the drying temperature from room temperature to a temperature around 135 °C, which was higher than the glass transition temperature of the blend.[12] Sample films of 0.2 mm thickness were prepared by

† Department of Polymer Chemistry.
‡ Department of Organic and Polymeric Materials.
[⊗] Abstract published in *Advance ACS Abstracts,* October 1, 1995.

0024-9297/95/2228-7514$09.00/0 

**Table 1. Sample Compositions and Phase-Volume Fractions of the PS-Rich Phase when Phase-Separated at 165° C**

| sample | $\phi_{PS} \times 100^a$ | $v_{PS}{}^b$ |
|---|---|---|
| PS40 | 39.9 | 0.34 |
| PS45 | 45.2 | 0.41 |
| PS54 | 54.3 | 0.54 |
| PS60 | 60.1 | 0.63 |
| PS65 | 65.0 | 0.70 |
| PS70 | 70.0 | 0.78 |
| PS75 | 75.0 | 0.85 |

[a] $\phi_{PS}$ = (volume of PS)/(volume of PS + volume of P2CS). [b] Calculated by eq 1.

annealing a pile of these thin films with a weight on top. The compositions of the samples used in this work are given in Table 1.

**Measurements.** The time-resolved light scattering (TRLS) measurements were performed with an instrument constructed in this laboratory. A He–Ne laser operating at a wavelength of 632.8 nm was used as a light source. The angular dependence of the scattered light intensity was measured by scanning a photomultiplier tube with a stepping motor, and the transmitted light intensity was monitored by a photodiode to make correction for the turbidity. The temperature jump to initiate phase separation was made by transferring a sample holder from a preheating block to a main copper block controlled at a desired temperature in the two-phase region to ±0.03 °C.

The morphological structure during phase separation was studied by observing the fractured surface of a specimen that was quenched after it was phase-separated for a desired period. Phase separation was made by keeping sample films in a thermostat, made of an aluminum block, controlled to ±0.03 °C. The block was placed in an atmosphere of nitrogen to suppress degradation of P2CS at high temperatures. The quick quench to a temperature well below the glass transition temperature was made by contacting both sides of the sample holder with two brass blocks that were cooled to −15 °C in a refrigerator. Since the grass transition temperature was much higher than room temperature, the morphological structure was observed at room temperature with a JEOL JSM-T220 electron microscope by detecting backscattered electrons. A clear compositional image was obtained in the electron micrograph without staining with dye. The area ratio of two separated phases in an electron micrograph was determined with a PIAS LA525 image analysis system.

## Results and Discussion

Figure 1 shows a plot of the fraction $v_{PS}$ of the volume of the PS-rich phase to the total volume of the blend phase-separated at 165 °C against the initial PS composition of the blend. The phase-volume fraction $v_{PS}$ was evaluated by image analysis of electron micrographs of the samples at the late stage of phase separation,[13] at which microdomains of coexisting compositions were already formed. The excess volume of mixing is generally negligible in polymer blends, and the volume fraction $\phi_{PS}{}^0$ of the initial blend can be expressed by using the volume fractions $\phi_{PS}{}^I$ and $\phi_{PS}{}^{II}$ of the two coexisting phases I and II by

$$\phi_{PS}{}^0 = v_{PS}\phi_{PS}{}^I + (1 - v_{PS})\phi_{PS}{}^{II} \quad (1)$$

within the framework of the quasi-binary approximation where the volume fraction of the plasticizer DBP was assumed to be constant in any phase. A good linear relation was obtained in Figure 1 as expected from eq 1, and the two coexisting compositions $\phi_{PS}{}^I$ and $\phi_{PS}{}^{II}$ were determined from the plot to be 0.83 and 0.17 by extrapolating the fitting line to $v_{PS} = 1$ and $v_{PS} = 0$.[14]

Figure 2 shows electron micrographs of the blends of various compositions phase-separated at 165 °C. The

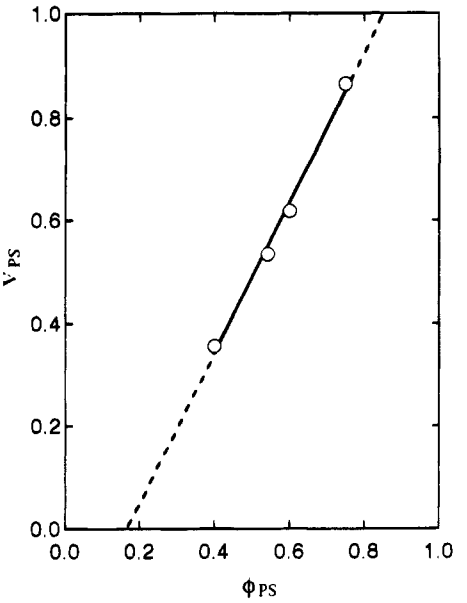


**Figure 1.** Plot of phase-volume fraction of polystyrene-rich phase $v_{PS}$ of samples phase-separated at 165 °C against the initial polystyrene volume fraction in the total polymer volume $\phi_{PS}$.

phase separation times were chosen so that the characteristic domain size, which was proportional to the inverse of the wavenumber giving the maximum intensity in the light scattering profile, became roughly 5 μm except for two blends of $\phi_{PS} = 0.40$ and 0.75. For these two compositions, which are far from the midpoint of the coexisting composition, electron micrographs for microdomains of characteristic size smaller than 5 μm were shown because of the very slow phase separation rates. As seen in the figure, a good contrast was obtained in the electron micrograph image because of the high electron density of chlorine atoms in P2CS. The brighter regions of the electron micrographs represent the P2CS-rich phase, and the darker regions represent the PS-rich phase.

In the neighborhood of the critical composition (samples PS54 and PS60) both phases formed continuous domains, and at compositions far from the critical composition (PS40 and PS75) the minority phase formed droplet domains in the background of the majority phase. These two morphological structures were already observed by various experiments.[1–5] In the intermediate ranges between these critical and off-critical compositions, cocontinuous domains and small droplets were found to coexist in the system as shown in the electron micrographs of PS45, PS65, and PS70. It is noted that the droplets were not dispersed uniformly among the cocontinuous domains but gathered in certain regions. The total volume of the regions occupied by the droplet domain structure was very large in PS70, indicating that the crossover from the cocontinuous domain to droplet structures was accomplished by increasing the fraction of the droplet structure regions.

The domain structure in the late stage of phase separation is believed to depend on the phase-volume fraction of the minority phase. When the volumes of the two separated phases are close (i.e., in the critical concentration region), microdomains connect and form the continuous structure, and when the volume of the minority phase is small compared with the volume of the majority phase (i.e., in the off-critical concentration region), microdomains of the minority phase cannot connect with each other and form droplets. The phase-

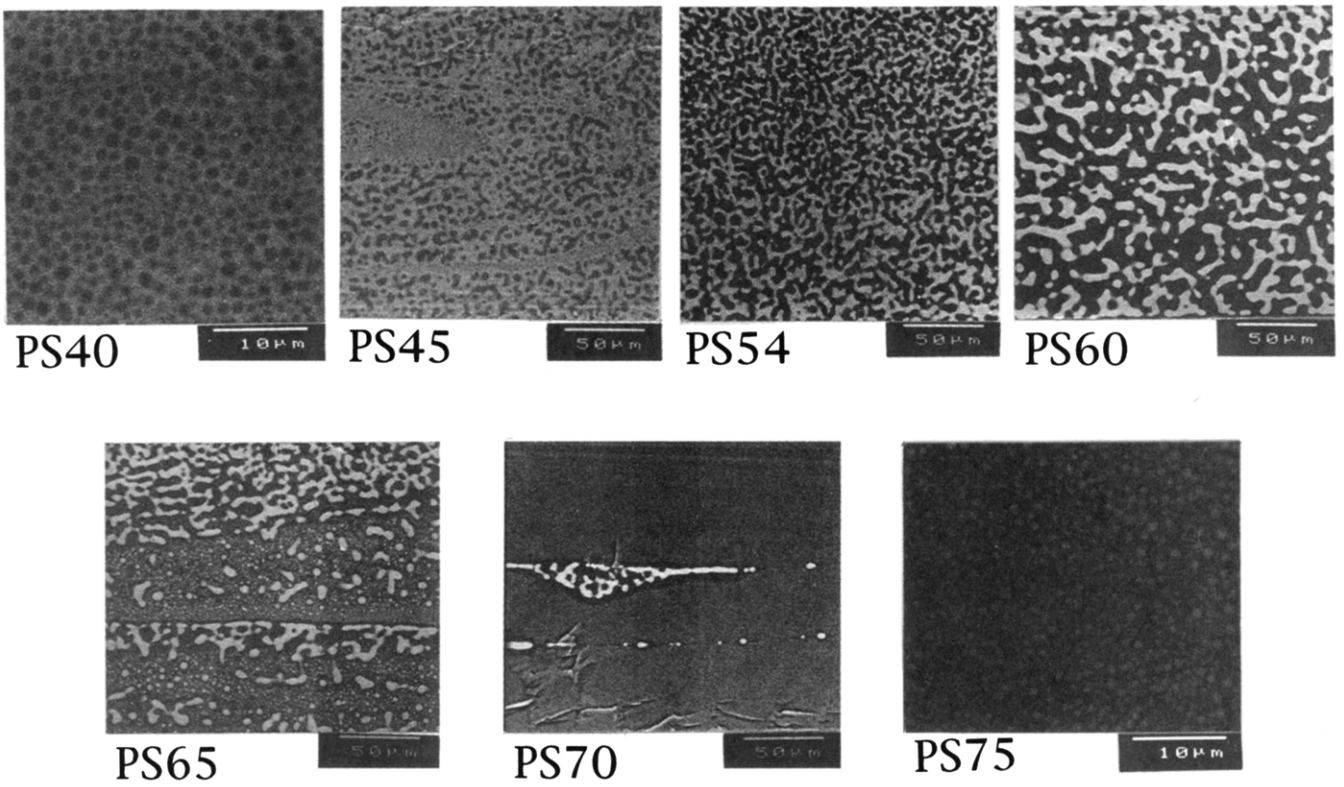


**Figure 2.** Electron micrographs (backscattered image) of the fractured surface of samples of different initial compositions phase-separated at 165 °C. Phase separation times were 17 (PS40), 1.8 (PS45), 1.8 (PS54), 2.1 (PS60), 1.8 (PS65), 1.8 (PS70), and 17 h (PS75). Brighter regions correspond to the P2CS-rich phase.

volume fractions calculated by eq 1 using the estimated coexisting volume fractions $\phi_{PS}^{I}$ and $\phi_{PS}^{II}$ are given in the third column of Table 1. The number of data points was not sufficient to determine the location and width of the crossover exactly. However, it was clearly indicated that the crossover was asymmetrical in the phase-volume fraction. The crossover on the PS-rich side of the phase diagram was located at a lower phase-volume fraction of the minority phase than the crossover on the P2CS-rich side, as described below. A uniform droplet structure was produced in PS40 where the phase-volume fraction of the minority phase $v_{minor}$ was 0.34, while the crossover domain structures were produced in PS65 and PS70 though their $v_{minor}$ (=0.30 and 0.22, respectively) were smaller than in PS40. Similarly, a uniform cocontinuous domain structure was observed at $v_{minor}$ = 0.37 (PS60) on the PS-rich side of the phase diagram, while a crossover structure was observed at $v_{minor}$ = 0.41 (PS45) on the other side. Therefore, whether the microdomains become droplets or cocontinuous domains is not determined only by phase-volume fractions. Recently, Tanaka[15] found that in the phase separation of the poly(vinyl methyl ether)/water system, the polymer-rich minority phase formed a network domain structure at fairly small phase volumes. This suggests that the viscosity of the minority phase is an important factor in determining the crossover composition.

The intensity of the light scattered from a blend under phase separation, which was measured by the time-resolved light scattering technique, showed a maximum in the wavenumber dependence. The maximum intensity increased and the location of the maximum shifted to smaller wavenumbers with a lapse of phase separation time. Figure 3 shows plots of the wavenumber $q_m$ giving the maximum intensity against the phase separation time $t$ in double-logarithmic scales for various blend compositions, and Figure 4 shows plots of the

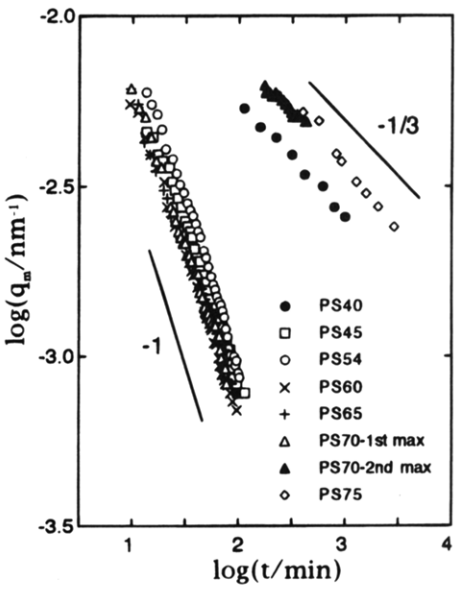


**Figure 3.** Double-logarithmic plots of wavenumber $q_m$ where the maximum was located in the scattered light intensity profile against phase separation time $t$ at 165 °C for different blend compositions.

maximum intensity $I_m$ against $t$.

At $\phi_{PS}$ = 0.54 and 0.60, where the cocontinuous domain structures were produced as already shown in Figure 2, the maximum scattered intensity $I_m$ and the characteristic wavenumber $q_m$ could be expressed by power relations[1-5]

$$q_m \sim t^{-\alpha} \tag{2}$$

$$I_m \sim t^{\beta} \tag{3}$$

in the late period of phase separation. The exponents

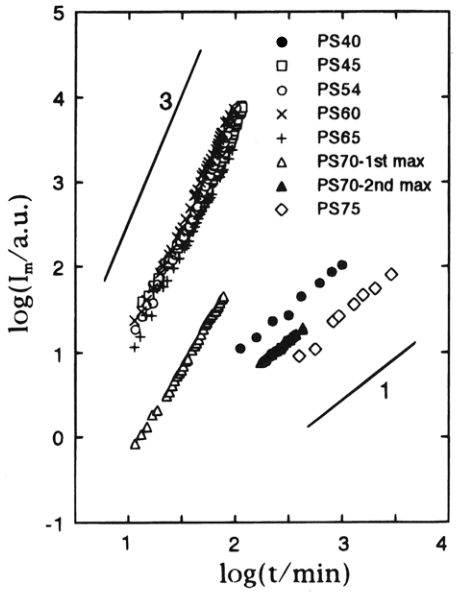


**Figure 4.** Double-logarithmic plots of maximum intensity $I_m$ against phase separation time $t$ at 165 °C for different blend compositions.

**Table 2. Exponents α and β of the Time Dependence of the Maximum Intensity and Characteristic Wavenumber**

| sample | α | | β | |
|---|---|---|---|---|
| PS40 | | 0.33 | | 1.04 |
| PS45 | 0.95 | | $3.1_0$ | |
| PS54 | $1.0_7$ | | $3.0_4$ | |
| PS60 | $1.0_0$ | | $2.9_0$ | |
| PS65 | $1.0_3$ | | $2.7_0$ | |
| PS70 | 0.96 | 0.33[a] | $2.2_0$ | 0.79[a] |
| PS75 | | 0.34 | | 1.09 |

[a] The second maximum.

were evaluated by the best fitting and are given in Table 2. The exponent α was very close to the value 1.0 theoretically predicted by Siggia[6] for the coarsening of cocontinuous domains in a fluid system. The exponent $\beta$ satisfied the relation $\beta/\alpha = 3$ within experimental accuracy, which indicates that phase separation reached the late stage. At $\phi_{PS} = 0.40$ and 0.75, where the droplet domains were produced, the maximum intensity $I_m$ and the characteristic wavenumber $q_m$ were also expressed by the power relations (eqs 2 and 3). The exponents, tabulated in Table 2, were very close to the values $\alpha = 1/3$ and $\beta = 1$ that were theoretically predicted for the coarsening of droplets.[7,8]

The curves representing the time evolution of the characteristic wavenumber $q_m$ for $\phi_{PS} = 0.45$, 0.65, and 0.70, where droplets and cocontinuous domains existed, approximately coincided with those for $\phi_{PS} = 0.54$ and 0.60, where only cocontinuous domains existed. For sample PS70, we continued the measurement over a long period and found that another maximum emerged at higher wavenumbers after the initially observed maximum shifted out of the lower limit of the measurable wavenumbers as shown in Figure 5. This second maximum was shifting very slowly and the time dependence of $q_m$ followed a 1/3 power law, as shown in Figure 3 and Table 2, in contrast to the linear time dependence of $q_m$ of the first maximum.

Similar results were obtained for the maximum intensity $I_m$ except the case of the first maximum of PS70. The $I_m$–$t$ curve for the crossover compositions $\phi_{PS} = 0.45$ and 0.65 coincided with the curves for the critical compositions $\phi_{PS} = 0.54$ and 0.60, and the second maximum of PS70 followed the same power relation as

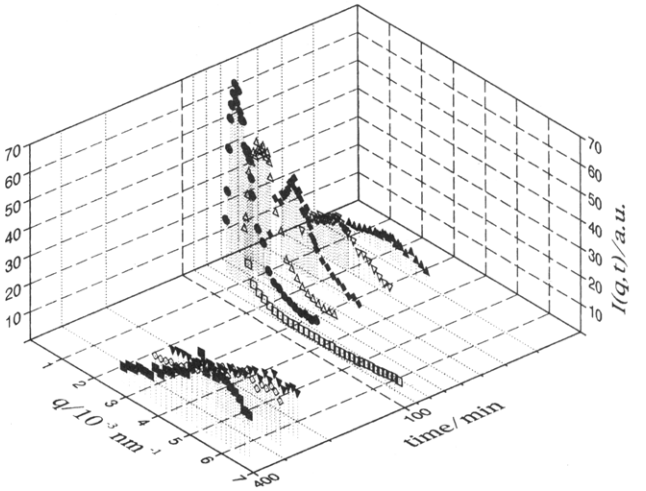


**Figure 5.** Time evolution of scattered light intensity profile at 165 °C for PS70. After an initially observed maximum shifted out of the lower limit of the measurable wavenumbers $q$, another maximum emerged at higher wavenumbers.

the maximum of the off-critical compositions did (see Table 2). However, the intensity of the first maximum of PS70 was much smaller than the maximum intensity of the other two samples of the crossover compositions compared at the same phase separation time. In addition, in the exponent $\beta$ for the samples of the critical and crossover compositions, only the exponent for the first maximum of PS70 was obviously smaller than 3.

The coincidence of the $q_m$–$t$ and $I_m$–$t$ curves for the crossover compositions $\phi_{PS} = 0.45$ and 0.65 with the curves for the critical compositions indicates that the maximum in the scattering profile observed for the crossover compositions was attributable to the scattering from the cocontinuous domains and that the coarsening mechanisms of the cocontinuous domains were hardly influenced by coexisting droplets. In other words, when cocontinuous domains and droplets coexisted, the scattering from cocontinuous domains was dominant over the scattering from droplets at least at the investigated period and wavenumbers. This is reasonable because the cocontinuous domains are coarsening much faster than droplets as indicated by the difference in the value of the exponent $\alpha = 1$ and 1/3 and consequently the characteristic size of the cocontinuous domains is much larger than the average spacing between droplets except in the very early period.

Although the time evolution of the intensity of the first maximum of PS70 deviated significantly from those of the samples of the critical compositions, the first maximum was attributed to the scattering from the cocontinuous domains as well, because the time dependence of $q_m$ of the first maximum coincided with those of the critical compositions and the length $L$, calculated by $L = 2\pi/q_m(t)$, was approximately the same size as the characteristic length of the continuous domains in the crossover domain structure observed at $t$. The deviation in the maximum intensity $I_m$ could be explained by the volume of the cocontinuous domains in the scattering volume: As seen in the electron micrograph of PS70 in Figure 2, the cocontinuous domains were localized in certain regions, and the total volume occupied by these regions, which was proportional to the scattering intensity, was very small. The deviation in the exponent $\beta$ might be similarly explained by the small total volume of cocontinuous domains. The maximum in the scattering profile reflects the periodic pattern of the cocontinuous domains. When the co-

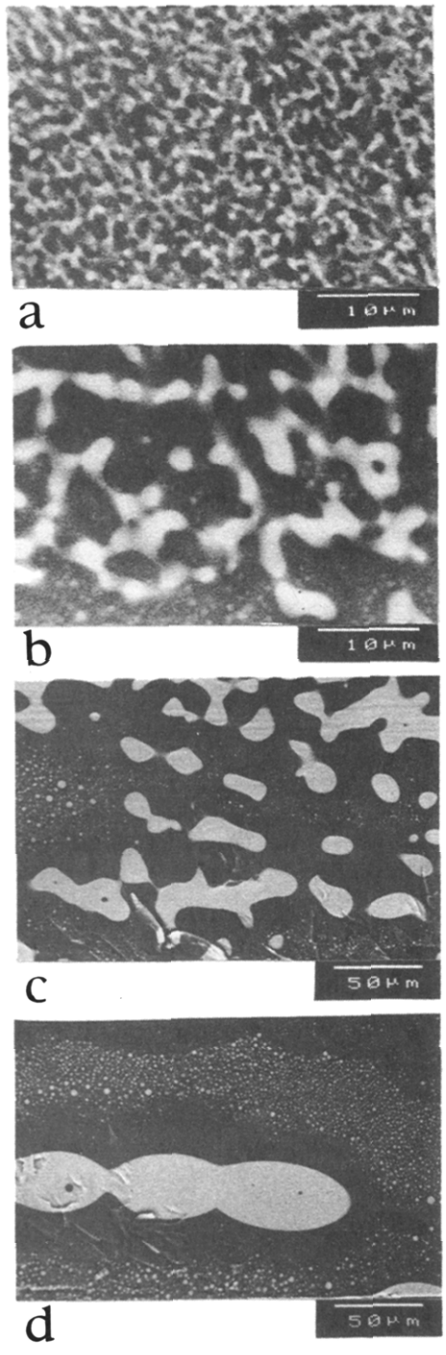


**Figure 6.** Electron micrographs of the fractured surface of PS65 samples phase-separated at 165 °C for (a) 0.5, (b) 1, (c) 8, and (d) 21 h.

continuous domains do not extend over the whole system and are localized in a region of finite volume, the scattering from the outermost layer of that region does not contribute to $I_m$. Since the volume of the outermost layer is increasing with the coarsening of the cocontinuous domains in that region, the volume of the inner part that contributes to the scattering at $q_m$ is gradually decreasing with time. As a consequence, the growth of the intensity would deviate from the 3.0 power relation, even when the coarsening was proceeding by Siggia's mechanism.

The second maximum observed in the scattering from PS70 was attributed to the scattering from the droplets surrounding the continuous domains. The values of the exponents $\alpha$ and $\beta$ indicated that the growth mechanism of the droplets was hardly influenced by coexisting cocontinuous domains. Therefore, both droplets and cocontinuous domains in the crossover structure were growing almost independently of the other domain structure.

Figure 6 shows the morphological structures of phase-separated domains of PS65 at different phase separation times. As already shown in Figure 2, at this composition the coexistence of cocontinuous domains and droplets was observed in the later period of phase separation. However, in the early period only cocontinuous domains were observed as seen in the electron micrograph at $t = 0.5$ h. At this phase separation time the maximum scattered intensity $I_m$ and the characteristic wavenumber $q_m$ did not satisfy the asymptotic power relations yet, and the ratio of the apparent exponents $\beta/\alpha$ was smaller than 3, which indicates that the phase separation did not reach the late stage at $t = 0.5$ h. In other words, droplets were generated in a period between the intermediate and late stages of phase separation. It is reasonable that only cocontinuous structures were observed in the early period. The crossover compositions are considered to be in the unstable region of the phase diagram and consequently phase separation proceeds through the spinodal decomposition in the early period of the phase separation. As long as the amplitude of composition fluctuations is smaller than the difference between the initial and the coexisting compositions, a cocontinuous structure typical for the spinodal decomposition should be produced.

At the late period, droplets of the P2CS-rich (minority in this case) phase were generated and coexisted with the cocontinuous domains. The droplets generated from the cocontinuous domains were obviously growing with time, and thus the pinning[16-18] associated with the percolation-to-cluster transition was not observed in the present system.

## References and Notes

(1) Binder, K. *Adv. Polym. Sci.* **1994**, *112*, 181; *Colloid Polym. Sci.* **1987**, *265*, 273.
(2) Hashimoto, T. *Phase Transitions* **1988**, *12*, 47.
(3) Nose, T. *Prog. Pacific Polym. Sci.* **1994**, *3*, 1; *Phase Transitions* **1987**, *8*, 245.
(4) Gunton, J. D.; Miguel, M. S.; Sahni, P. S. *Phase Transitions and Critical Phenomena*; Academic Press: New York, 1983; Vol. 8, p 267.
(5) Furukawa, H. *Adv. Phys.* **1985**, *34*, 703.
(6) Siggia, E. D. *Phys. Rev. A* **1979**, *20*, 595.
(7) Binder, K.; Stauffer, D. *Phys. Rev. Lett.* **1974**, *33*, 1006.
(8) Lifshitz, I. M.; Slyozov, V. V. *J. Phys. Chem. Solids* **1961**, *19*, 35.
(9) Okada, M.; Kwak, K. D.; Chiba, T.; Nose, T. *Macromolecules* **1993**, *26*, 6681.
(10) Alexandrovich, P. S.; Karasz, F. E.; MacKnight, W. J. *J. Macromol. Sci., Phys.* **1980**, *B17*, 501.
(11) Chu, B.; Linliu, K.; Ying, Q.; Nose, T.; Okada, M. *Phys. Rev. Lett.* **1992**, *68*, 3184.
(12) Kwak, K. D.; Okada, M.; Nose, T. *Polymer* **1991**, *30*, 864.
(13) Kwak, K. D.; Okada, M.; Chiba, T.; Nose, T. *Macromolecules* **1992**, *25*, 7204.
(14) See ref 13 for the validity of the present method of evaluating coexisting compositions.
(15) Tanaka, H. *Macromolecules* **1992**, *25*, 6377.
(16) Kotnis, M. A.; Muthukumar, M. *Macromolecules* **1992**, *25*, 1716.
(17) Hashimoto, T.; Takenaka, M.; Izumitani, T. *J. Chem. Phys.* **1992**, *97*, 679; **1993**, *98*, 3523.
(18) Läuger, J.; Lay, R.; Gronski, W. *J. Chem. Phys.* **1994**, *101*, 7181.

MA950756W